SIMILARITIES AND DIFFERENCES BETWEEN $\bar{p}p$ AND pp SCATTERING AT TeV ENERGIES AND BEYOND

Pierre GAURON and Basarab NICOLESCU

Division de Physique Théorique*, Institut de Physique Nucléaire,
91406 Orsay Cedex, France
and Laboratoire de Physique Théorique des Particules Elémentaires,
Université Pierre et Marie Curie, 75252 Paris Cedex 05, France

and

Elliot LEADER

Birkbeck College, University of London, London WC1E, United Kingdom

IPNO/TH 88-55 DECEMBER 1988

* Laboratoire Associé au C.N.R.S.

ABSTRACT

The significant difference between the pp and $\bar{p}p$ elastic $d\sigma/dt$ discovered at the CERN ISR, and the behaviour of the $\bar{p}p$ $d\sigma/dt$ at the CERN collider, which have profound implications for the asymptotic behaviour of hadron scattering amplitudes, are explained in terms of a model theory based upon general S-matrix principles and a dynamical assumption of "maximal strength" for the strong interactions. Our model theory provides an excellent description of the pp and $\bar{p}p$ data in the huge range $10 \leq \sqrt{s} \leq 630$ GeV for $|t| \leq 2.5$ $(\text{GeV})^2$. Several striking consequences of the theory will be testable at Tevatron energies and beyond.

1. INTRODUCTION

There is convincing "posthumous" evidence from the ISR for a striking difference of shape between pp and $\bar{p}p$ differential cross-sections at the highest ISR energies [1]. Moreover the behaviour of $\bar{p}p$ seen at the CERN $Sp\bar{p}S$ collider [2-3] seems to represent a smooth extrapolation of the shape and structure of the ISR $\bar{p}p$ data, but not of the ISR pp data.

The significant difference between pp and $\bar{p}p$ at ISR energies rules out most of the existing models of diffractive scattering.

It seems likely that pp and $\bar{p}p$ will be different even at CERN-collider and TeV energies, and, as we shall argue, it is quite feasible that they will remain different for ever.

This, of course, is quite surprising (though some suggestions for such behaviour were aired in the literature long ago [4]) and contrary to the widely held belief that the annihilation channels, which are largely responsible for the huge difference between pp and $\bar{p}p$ at low energies, should become less and less important as the energy increases.

In fact, within the framework of present day field theories or rigorous treatments of the mathematical properties of scattering amplitudes, there is absolutely no general reason why pp and $\bar{p}p$ should not continue to differ as $s \to \infty$. Indeed, we shall suggest that there is a rich and interesting structural difference between pp and $\bar{p}p$ at all energies, and it will be a challenge for the Tevatron and future accelerators like the SSC to discover what, in reality, Nature chooses.

It is a challenge also to field theories like QCD to provide theoretical answers, but these will be very hard to achieve since they will demand calculations in the non-perturbative regime.

In this paper we provide a theoretical framework for interpreting these new experimental results. Because we are unable to carry out a fundamental theoretical calculation of the scattering amplitudes in the kinematic region of interest, we are forced to construct a *model* theory which, we believe, reflects certain characteristics that will eventually emerge from a more fundamental theory.

It is based upon :

a) Compatibility with general principles and the constraints of the rigorous asymptotic theorems, and in addition,

b) A formulation of the "principle of maximal strength of strong interactions" i.e. a dynamical assumption that the strong interactions are (in a sense that is spelled out in detail in sect. 3), "as strong as they can possibly be"[*].

The implementation of these ideas provides us with a certain mathematical picture of the scattering amplitudes at very high energies. This picture, when combined with the above mentioned data, leads to the following interesting and somewhat unconventional predictions for the asymptotic behaviour of pp and $\bar{p}p$:

i) The total cross-section difference $\Delta\sigma$ does not tend to zero. It has a *minimum* in the region $\sqrt{s} \simeq 100$ GeV *and then* rises slowly like $\ln s$ as $s \to \infty$;

ii) The ratio ρ of real to imaginary parts in the forward direction does not tend to zero. In fact $\rho_{\bar{p}p}$ is predicted to change sign and ultimately

---

[*] Recent phenomenological studies concerning this principle are quoted in ref. [5].

$$\rho_{pp} \to -\rho_{\bar{p}p} \to \cong \text{const} \quad \text{as } s \to \infty \ ; \tag{1.1}$$

iii) For values of t not only inside but also outside the diffraction peak

$$\frac{(d\sigma/dt)^{\bar{p}p}}{(d\sigma/dt)^{pp}} \to 1, \text{ as } s \to \infty , \tag{1.2}$$

however

$$\frac{d\sigma}{dt}^{\bar{p}p} - \frac{d\sigma}{dt}^{pp} \not\to 0 \ ; \tag{1.3}$$

iv) Inside the dip region the structure of $d\sigma/dt$ gets richer as the energy increases and $(d\sigma/dt)^{\bar{p}p} - (d\sigma/dt)^{pp}$ has an increasing number of oscillations as a function of t as s increases ;

v) For t values beyond (and not too far from) this structure region, $d\sigma/dt$ for both pp and $\bar{p}p$ grows steadily with energy. This property distinguishes our approach from other published models [6-7] which attempt to describe the experimental difference between pp and $\bar{p}p$, and will be testable at Tevatron energies and beyond ;

vi) The ratio of elastic to total cross-sections, which seemed constant at ISR energies, and which grows between ISR and CERN-collider energies for $\bar{p}p$, will continue to vary very slowly with energy and gradually tends to a limiting non-zero value;

vii) If "asymptopia" is the region where the limits (ii) and (vi) are attained, then it is very far away indeed. Thus, for the crossing-even amplitude, which controls the region of very small t, the asymptotically growing pieces to-

tally dominate at astronomically high energies. Nevertheless there is no "desert" : the asymptotic terms in the crossing-even amplitude induce finite-energy effects (e.g. the increase of total cross-sections); moreover for the crossing-odd amplitude, which controls the region of t beyond the diffraction dip at high energies, the asymptotically growing pieces are already dominant at ISR energies. Consequently, the region of very high energies remains full of interest and it can be particularly well explored by accelerators which have both a pp and a $\bar{p}p$ facility at similar energies. (This is an important matter to bear in mind for the future SSC).

The plan of our paper is as follows. In sect. 2 we recall some of the general principles governing the asymptotic behaviour of scattering amplitudes. In sect. 3 we present a model theory for the asymptotic part of the amplitudes and enunciate the principle of maximal strength for the strong interactions. In sect. 4 we analyze some consequences of this hypothesis at very high energies. The complete form of our amplitudes is presented in sect. 5. In sect. 6 we compare our model theory with a wide range of data on the pp and $\bar{p}p$ reactions. Predictions and tests of our picture at Tevatron and higher energies are presented in sect. 7 and in sect. 8 we comment upon certain other theoretical approaches to very high-energy nucleon-nucleon scattering. Our conclusions follow in sect. 9.

2. USE AND MISUSE OF ASYMPTOTIC THEOREMS

Several powerful and rigorous theorems exist concerning the asymptotic behaviour of scattering amplitudes. They are based on very general principles and reasonable sounding assumptions and also take account, at least partially, of the constraints due to unitarity. All serious models or theories should respect them.

The theorems are usually stated by their authors in careful mathematical terms and with a clear indication of the underlying assumptions ⁑ . These aspects are often overlooked or simplified in practical use and this can lead, in some cases, to quite false statements.

Two cases are highly germane to our study :

1) The original "Pomeranchuk theorem" [9] proved that

$$\Delta\sigma \equiv \sigma_T^{\bar{p}p} - \sigma_T^{pp} \to 0, \text{ as } s \to \infty . \tag{2.1}$$

However there are physical assumptions underlying this theorem, namely that $\sigma_T^{\bar{p}p}$ and σ_T^{pp} tend to constant values as $s \to \infty$, which are questionable in the light of our present knowledge of the behaviour of cross-sections and scattering amplitudes.

The acceptable modern version of this theorem [10], given that cross-sections may be growing indefinitely, claims that

$$\frac{\sigma_T^{\bar{p}p}}{\sigma_T^{pp}} \to 1, \text{ as } s \to \infty \tag{2.2}$$

which is not at all the same as demanding $\Delta\sigma \to 0$, as can be seen from the trivial example

$$\begin{aligned} \sigma_T^{pp} &= A.\ln^2 s + B \\ \sigma_T^{\bar{p}p} &= A \ln^2 s + C \end{aligned} \tag{2.3}$$

with $B \neq C$.

⁑ For a recent review of asymptotic theorems see ref. [8].

ii) The Cornille-Martin theorem [11] is often misquoted as simply showing that

$$\frac{d\sigma}{dt}^{\bar{p}p} = \frac{d\sigma}{dt}^{pp} \quad , \text{ as } s \to \infty \tag{2.4}$$

whereas actually it proves that

$$\frac{(d\sigma/dt)^{\bar{p}p}}{(d\sigma/dt)^{pp}} \to 1, \text{ as } s \to \infty \tag{2.5}$$

which is not at all the same as (2.4) (by analogy with (2.2) and (2.3) above). Moreover the proof holds only inside the diffraction peak, a region that is probably shrinking like const $/\ln^2 s$. (In fact, the rigorous statement is that the ratio in (2.5) contains unity among its limiting values).

A further point worth stressing is that asymptotic theorems are statements about limits as $s \to \infty$. They are not direct statements about present day energies and they are most useful as "boundary conditions" in constructing model theories.

Thus ever since the first great ISR discovery in 1973 that the proton-proton total cross-section seemed to be growing like $\ln^2 s$ is has been tantalizing to suppose that strong interaction total cross-sections do really saturate the Froissart-Martin bound [12]

$$\sigma_T \leqslant \text{const} \cdot \ln^2 s, \text{ as } s \to \infty \, . \tag{2.6}$$

The constant in (2.6) is obviously positive and can be shown rigorously [13] to be bounded by

$$\text{const} \leqslant \frac{\pi}{2 m_\pi^2} \approx 60 \text{ mb} \, . \tag{2.7}$$

It should be stressed that, in contrast with the bound (2.6), the bound (2.7) only takes elastic unitarity into account and can probably be much improved. Phenomenulogically the coefficient of $\ln^2 s$ is found to be $\simeq 0.4$ mb, much lower than the upper bound (2.7). This does not mean that the growth is not maximal in the functional sense. As was explained for example in ref.[4], an asymptotic $\ln^2 s$ behaviour is perfectly compatible with any value $0 < \text{const} \leq \pi/m_\pi^2$. We shall regard the phenomenological $\ln^2 s$ increase of both pp and $\bar{p}p$ total cross-sections as an indication for "maximal functional growth" (2.6) of the strong interaction total cross-sections. Our amplitudes will be constructed to have this asymptotic behaviour.

Once it is accepted that total cross-sections have $\ln^2 s$ growth asymptotically, it follows rigorously that $\Delta\sigma$ need not tend to zero. Instead one has only the bound [14]

$$|\Delta\sigma| \leq \text{const} \cdot \ln s, \text{ as } s \to \infty . \tag{2.8}$$

As mentioned above, there has long been a general awareness of the possibility of continuously growing total cross-sections. The idea that $|\Delta\sigma|$ can grow indefinitely is much less widely appreciated. But we shall argue below that the new data on $d\sigma/dt$ referred to in the Introduction are nicely compatible with a picture in which also $|\Delta\sigma|$ eventually grows functionally as fast as it is permitted to i.e. like $\ln s$ asymptotically.

Linked to these considerations is the rigorous fact that the ratio ρ, of the real to imaginary parts of the forward scattering amplitude, need not tend to zero asymptotically. Indeed it can be shown rigorously that one can perfectly

well have $\rho_{pp} \to$ const and $\rho_{\bar{p}p} \to$ const as $s \to \infty$, which is compatible with our analysis of the data mentioned in the Introduction.

A word of caution is necessary about the use of a condition (based on a theorem of Fischer et al. [15]) relating the behaviour of the ratio of real to imaginary parts of the crossing-odd amplitude to the behaviour of $\Delta\sigma$ as $s \to \infty$. The assumptions underlying this theorem explicitly exclude a wide class of acceptable behaviours in which $\Delta\sigma \not\to 0$ asymptotically, and there is no general reason for insisting upon these relations (in a recent paper, Fischer also has formulated appropriate theorems for the latter case [16]).

3. A MODEL THEORY FOR ASYMPTOTIC BEHAVIOUR

We construct amplitudes for high energy pp and $\bar{p}p$ scattering, which respect all the relevant rigorous general asymptotic bounds. They are designed to saturate the growth bounds functionally. We refer to this as the principle of maximal growth for the strong interactions [4]*.

We ignore the spin degrees of freedom and utilize spin-averaged amplitudes F_{pp}, $F_{\bar{p}p}$ normalized so that

$$\frac{d\sigma}{dt} = \frac{1}{16\pi s^2} |F(s,t)|^2,$$

$$\sigma_T = \frac{1}{s} \operatorname{Im} F(s,0), \tag{3.1}$$

$$\Delta\sigma = \frac{1}{s} [\operatorname{Im} F_{\bar{p}p}(s,0) - \operatorname{Im} F_{pp}(s,0)].$$

We break up our amplitudes into two pieces (F_+, F_-) even and odd under crossing respectively with

---

* An analogous principle, relevant to the case of constant total cross-sections, can be found in ref. [17].

$$F_{pp} = F_+ + F_- ,$$
$$F_{\bar{p}p} = F_+ - F_- . \qquad (3.2)$$

We then separate $F_\pm$ into a "normal" part $F_\pm^N$ and an asymptotic part $F_\pm^{AS}$ which, having maximal growth, dominates ultimately. For $t = 0$ and $s \to \infty$ we have

$$F_+^{AS} \to i\, s\, F_1[\ell n(se^{-i\pi/2})]^2$$
$$\simeq s\, F_1[i\, \ell n^2 s + \pi\, \ell n\, s], \qquad (3.3)$$

$$F_-^{AS} \to s\, O_1[\ell n(se^{-i\pi/2})]^2$$
$$\simeq s\, O_1[-i\pi\, \ell n\, s + \ell n^2 s] , \qquad (3.4)$$

where F_1 and O_1 are constants and we refer to the asymptotic behaviour in (3.3) and (3.4) as "Froissaron" and "odderon" type behaviour respectively. (The reversal of the roles of real and imaginary parts between (3.3) and (3.4) should be noted.)

Eqs. (3.3)-(3.4) represent the asymptotic growth at $t=0$. The t-dependence permitted away from the forward direction is then non-trivial and non-arbitrary. It is controlled by the Auberson-Kinoshita-Martin (AKM) theorem [18] according to which, as $s \to \infty$

$$F_+(s,t) \to F_+(s,0)\, g_+(\tau) ,$$
$$F_-(s,t) \to F_-(s,0)\, g_-(\tau) , \qquad (3.5)$$

where $g_\pm(\tau)$ are entire functions of order 1/2 of τ^2 and τ is the scaling variable

$$\tau = \text{const} \cdot \sqrt{-t} \cdot \ell n\, s \qquad (3.6)$$

Thus the t-behaviour and s-behaviour are inextricably linked for amplitudes with this growth. It follows trivially, for example, that asymptotically the diffraction peak must shrink like const/$\ell n^2 s$. though this behaviour may only show itself at ultra-high energies when the asymptotic parts of the amplitude begin to dominate.

In order to construct amplitudes that conform to the AKM theorem, we have found it useful to turn to the complex J-plane. The imaginary parts of the asymptotic contributions $F_{\pm}^{AS}(s,t)$ are expressed in terms of the t-channel partial wave amplitudes $f_{\pm}(J,t)$ via the Sommerfeld-Watson transform. At $t = 0$ the maximal behaviour in (3.3) and (3.4) corresponds to a triple pole and a double pole at $J = 1$ in $f_{\pm}(J,0)$ respectively. For $t \neq 0$ we have chosen the simplest possible t-dependent J-plane singularities that we can think of, which reduce at $t = 0$ to the required triple and double poles. These produce, via the Sommerfeld-Watson transform, functions of s and t which possess the AKM asymptotic form (3.5).

We have thus taken

$$f_+(J,t) = \frac{\beta_+(J,t)}{[(J-1)^2 - tR_+^2]^{3/2}} \qquad (3.7)$$

and

$$f_-(J,t) = \frac{\beta_-(J,t)}{(J-1)^2 - tR_-^2}\,, \qquad (3.8)$$

where $R_{\pm}$ are real positive constants. The residue functions $\beta_{\pm}(J,t)$ are assumed to be slowly varying functions of J and to have a simple exponential t-dependence.

The function in (3.7) has branch cuts for $t \neq 0$ which are taken to lie along

$$\text{Re } J = 1, \quad \sqrt{-t}\, R_+ \leq \text{Im } J \leq \infty$$

and (3.9)

$$\text{Re } J = 1, \quad -\infty \leq \text{Im } J \leq -\sqrt{-t}\, R_+ .$$

The usual Sommerfeld-Watson contour can be distorted so as to run along the branch cuts and we are finally left with integrals of the discontinuity of the function (3.7) across the branch cuts, of the general form

$$\frac{1}{2i\pi} \int_{1-i\infty}^{1+i\infty} dJ \; \text{Disc} \left\{ \frac{s^J \beta_+(J,t)}{[(J-1)^2 - tR_+^2]^{3/2}} \right\} . \tag{3.10}$$

For the crossing-odd amplitude the function in (3.8) has a pair of complex conjugate moving poles at

$$J = 1 \pm i\sqrt{-t}\, R_- \tag{3.11}$$

and the Sommerfeld-Watson integral is then trivial.

For the residue functions $\beta_\pm(J,t)$, we make a Taylor expansion around $J = 1$, keeping as many terms as we can without rendering the integrals divergent i.e. we put

$$\beta_+(J,t) = \beta_0(t) + (J-1)\beta_1(t) + (J-1)^2\beta_2(t) , \tag{3.12}$$

$$\beta_-(J,t) = \tilde{\beta}_0(t) + (J-1)\tilde{\beta}_1(t) . \tag{3.13}$$

The functions $\beta_1(t)$, $\tilde{\beta}_1(t)$ will be taken as exponentials for simplicity. Then the integrals involved in $F_\pm$ are essentially Mellin transforms and can be evaluated analytically.

The real parts of the functions $F_\pm(s,t)$ are constructed by demanding that the correct crossing properties under $s \to e^{i\pi}s$ hold asymptotically i.e. we require that

$$F_{\pm}^{AS}(e^{i\pi}s,t) = \pm[F_{\pm}^{AS}(s,t)]^{*} . \tag{3.14}$$

Carrying out the Mellin transforms, using (3.12) and (3.13) and imposing (3.14), we arrive at the following form for $F_{\pm}^{AS}(s,t)$:

$$\frac{1}{is}F_{+}^{AS}(s,t) = F_1 \ell n^2\tilde{s}\,\frac{2J_1(R_+\tilde{\tau})}{R_+\tilde{\tau}}e^{b_1^+t} + F_2 \ell n\tilde{s}\,J_0(R_+\tilde{\tau})e^{b_2^+t}$$

$$+ F_3[J_0(R_+\tilde{\tau}) - R_+\tilde{\tau}J_1(R_+\tilde{\tau})]e^{b_3^+t}, \tag{3.15}$$

$$\frac{1}{s}F_{-}^{AS}(s,t) = O_1 \ell n^2\tilde{s}\,\frac{\sin(R_-\tilde{\tau})}{R_-\tilde{\tau}}e^{b_1^-t} + O_2 \ell n\tilde{s}\,\cos(R_-\tilde{\tau})e^{b_2^-t} + O_3e^{b_3^-t} \tag{3.16}$$

where J_n are Bessel functions, F_k, O_k, $b_k^{\pm}$ (k=1,2,3) are constants,

$$\tilde{s} = \frac{s}{s_0}e^{-i\pi/2} \text{ , with } s_0 = 1 \text{ GeV}^2 , \tag{3.17}$$

and $\tilde{\tau}$ is the crossing-symmetric version of the AKM scaling variable

$$\tilde{\tau} = (-\frac{t}{t_0})^{1/2}\ell n\tilde{s}, \quad \text{with } t_0 = 1 \text{ GeV}^2 . \tag{3.18}$$

The existence of the term $O_3e^{b_3^-t}$ in $F_-^{AS}(s,t)$ does not, strictly speaking, follow from our previous arguments, since its imaginary part is zero for all t. Nonetheless it is allowed analytically and is the natural subsequent term in a decreasing sequence of powers of ln s. A term of this kind has been referred to in the literature as the "minimal" or "zeroth order" odderon [19].

From (3.15) and (3.16) we see that at t=0 we obtain terms with the following s-dependance :

$$\text{in Im } F_+^{AS}(s,0) : s\ \ell n^2 s,\ s\ \ell n\ s,\ s, \tag{3.19}$$

$$\text{in Im } F_-^{AS}(s,0) : s\ \ell n\ s,\ s. \tag{3.20}$$

It is seen that our assumption of simplicity in the complex J-plane leads to the expected "Froissaron" and "odderon" behaviour, as well as to additional terms growing less rapidly with s at t=0. These terms are nonetheless important at t≠0 as will be discussed in sect. 7. Of these the term growing like s in $\text{Im } F_+^{AS}(s,0)$ should not be thought of as the t=0 manifestation of a Regge Pomeron . Its t-dependance is linked to its s-dependence in a way which is not characteristic of the usual Pomeron.

4. HIGH ENERGY BEHAVIOUR DUE TO THE ASYMPTOTIC AMPLITUDES

The asymptotic amplitudes $F_\pm^{AS}(s,t)$ given in (3.15) and (3.16) possess several interesting properties which have unusual phenomenological consequences which we list below.

Beware that these are asymptotic properties and that we do not really understand the origin of the energy scales of the strong interactions. The only natural scale would seem to be the energy corresponding to typical hadron masses , yet we know that new effects begin to show themselves at the lowest ISR energies i.e. for c.m. energies $\sqrt{s} \gtrsim 20$ GeV. Thus our asymptotic statements are not expected to be literally valid at CERN-collider energies where our numerical studies (see sect. 6), including the "normal" amplitudes, indicate a considerable residue of non-asymptotic behaviour in F_+ for small t. To understand the behaviour to be expected up to a few tens of TeV one must have recourse to the numerical results.

i) One interesting feature is the non-uniformity of the behaviour as $s \to \infty$ at fixed t.

For example, at t=0 the ultimately dominant terms are such that

$$F_+^{AS}(s,0) \to i\, F_1 s\, \ell n^2 s\ ,$$
$$F_-^{AS}(s,0) \to 0_1 s\, \ell n^2 s\ , \qquad (4.1)$$

whereas for any fixed $t \neq 0$ one finds from (3.15)-(3.16)

$$F_+^{AS}(s,t) \to is\sqrt{\ell n\, s}\ h_+(s,t)\ ,$$
$$F_-^{AS}(s,t) \to s\ \ell n\, s\ h_-(s,t)\ , \qquad (4.2)$$

where $h_\pm$ are bounded oscillating functions.

So for $t \neq 0$ and fixed, it is actually F_- that eventually dominates. In practice our numerical studies indicate that for small t, i.e. $|t| \lesssim 0.6\ \text{GeV}^2$, F_- is still small at collider energies, but for $|t| \gtrsim 1.2\ \text{GeV}^2$ F_- already dominates at the collider.

Of course these considerations are somewhat academic near the forward direction since physics can never distinguish between $t=0$ and t infinitesimally small, but it does mean that for t significantly different from zero the asymptotic growth is quite different from that in the forward direction.

ii) As $s \to \infty$

$$\overset{\sim}{\tau} \to \tau \equiv \text{Re}\ \overset{\sim}{\tau} = \left(-\frac{t}{t_0}\right)^{1/2} \ell n\, s \qquad (4.3)$$

and the differential cross-section $d\sigma/dt$ approaches the AKM form for τ fixed as $s \to \infty$:

$$\frac{d\sigma}{dt} \to \ell n^4 s \cdot g(\tau)\ . \qquad (4.4)$$

That is to say that a plot of $(1/\ell n^4 s)\ d\sigma/dt$ vs τ will ultimately settle down to a universal scaling shape $g(\tau)$.

Considered as a function of t the picture is quite different. The position of the diffraction dip is controlled by the functions $J_1(R_+\bar{\tau})$ and $\sin(R_-\bar{\tau})$. Say it occurs at $\tau = \tau_{dip}$. Then in a plot vs t the dip will occur at

$$t = t_{dip} = -\, t_0 \frac{\tau_{dip}^2}{\ell n^2 s} \qquad (4.5)$$

i.e. at a value of t that tends to zero like $1/\ell n^2 s$. In other words, in a plot of $d\sigma/dt$ vs t, the diffraction peak will ultimately shrink like $1/\ell n^2 s$.

iii) For t values inside the diffraction peak or for fixed τ, we have

$$\left(\frac{d\sigma}{dt}\right)^{pp} = (\mathrm{Im}\, F_+^{AS})^2 + (\mathrm{Re}\, F_-^{AS})^2 + \ldots \qquad (4.6)$$

and

$$\left(\frac{d\sigma}{dt}\right)^{\bar{p}p} = (\mathrm{Im}\, F_+^{AS})^2 + (-\mathrm{Re}\, F_-^{AS})^2 + \ldots \qquad (4.7)$$

so that

$$\frac{(d\sigma/dt)^{\bar{p}p}}{(d\sigma/dt)^{pp}} \to 1 \qquad (4.8)$$

for τ fixed or t inside the diffraction peak and $s \to \infty$, as demanded by the Cornille-Martin theorem [11]. Of course, the difference

$$\Delta\left(\frac{d\sigma}{dt}\right) \equiv \left(\frac{d\sigma}{dt}\right)^{\bar{p}p} - \left(\frac{d\sigma}{dt}\right)^{pp} \qquad (4.9)$$

does not tend to zero since the less dominant terms left out in (4.6)-(4.7) grow with s, even inside the diffraction peak.

The result (4.8) is demanded by very general arguments and is respected by, but is not at all specific to, our model theory. What is surprising is that we find that

$$\frac{(d\sigma/dt)^{\bar{p}p}}{(d\sigma/dt)^{pp}} \to 1 \quad , \; t \text{ fixed}, \; s \to \infty \tag{4.10}$$

for any fixed t and therefore not just for t-values inside the diffraction peak. Once again (4.10) does not imply that $\Delta(d\sigma/dt)$ tends to zero. Our numerical studies show that this difference has a lot of structure in the region of the diffraction dip and that this structure gets richer as s increases.

iv) Although the difference of the total cross-sections ultimately behaves like

$$\Delta\sigma \to 2\pi\, O_1 \, \ell n\, s \quad , \text{ as } s \to \infty \, , \tag{4.11}$$

in practice $\Delta\sigma$ first decreases to a minimum at $\sqrt{s} \simeq 100$ GeV before beginning to grow (see sect. 6).

v) For the ratio of real to imaginary parts in the forward direction one has, because of (3.2) and (4.1) that, as $s \to \infty$

$$\rho_{pp} \to \frac{\mathrm{Re}\, F_-^{AS}(s,0)}{\mathrm{Im}\, F_+^{AS}(s,0)} \to \frac{O_1}{F_1} \tag{4.12}$$

and

$$\rho_{\bar{p}p} \to \frac{-\mathrm{Re}\, F_-^{AS}(s,0)}{\mathrm{Im}\, F_+^{AS}(s,0)} \to -\frac{O_1}{F_1} \quad . \tag{4.13}$$

Hence the remarkable result that

$$\rho_{pp} = -\rho_{\bar{p}p} = \text{const} \neq 0, \text{ as } s \to \infty \, . \tag{4.14}$$

vi) The difference (4.9) of the differential cross-sections is given, at t=0, by

$$8\Delta\left(\frac{d\sigma}{dt}\right)(s,t=0) = (F_2O_1 - F_1O_2)\,\ell n^2 s + 2\,(F_3O_1 - F_1O_3)\,\ell n\, s$$

$$+ (F_3O_2 - F_2O_3) + \frac{\pi^2}{2}(F_2O_1 - F_1O_2) + \ldots \tag{4.15}$$

The numerical results suggest that the coefficient of the term in $\ell n^2 s$ is almost zero.

vii) Finally we note an interesting constraint on the Froissaron and odderon parameters arising from the obvious relation

$$\sigma_{el} \leq \sigma_T \ . \tag{4.16}$$

Consider the limit s arbitrary large but fixed, $t \to 0$ and therefore $\tau \to 0$. Because of the AKM properties of $F_\pm$ amplitudes they can be expanded about $\tau = 0$. It is then easy to establish the following inequality

$$\frac{t_0}{16\pi} \frac{(F_1^2 + O_1^2)^2}{F_1(\frac{1}{4} F_1^2 R_+^2 + \frac{1}{3} O_1^2 R_-^2)} \leq \frac{\sigma_{el}}{\sigma_T} \ . \tag{4.17}$$

The formulae (4.16)-(4.17) indicate that $R_\pm$ can not be arbitrary for given F_1 and O_1. For the realistic case $O_1 \ll F_1$ (see section 6 and Table I), (4.16)-(4.17) lead to a lower bound for R_+ in terms of F_1.

5. PARAMETRIZATION OF THE SCATTERING AMPLITUDES

We explained in sect. 3 how our amplitudes $F_\pm$ are separated into a "normal" part $F_\pm^N$ and an asymptotic part $F_\pm^{AS}$ which dominates as $s \to \infty$. The $F_\pm^{AS}$ were defined and discussed in sects. 3 and 4. We turn now to the structure of $F_\pm^N$.

As mentioned in sect. 4 the only obvious energy scale for the strong interaction is that of the hadron masses. In consequence we do not think it is meaningful or useful to define "high energies" as the energy regime of the most recent accelerators. Thus, to carry out an analysis of data limited to that regime only is, in our opinion, misleading and lacking in physical justification.

Our study on the contrary will encompass pp and $\bar{p}p$ data for <u>all</u> energies beyond $\sqrt{s}$ = 10 GeV.

To handle this huge range of energies and vast amount of data, we shall have recourse to standard Regge theory in constructing $F_\pm^N$. Although Regge theory per se is no longer much in vogue it does represent a fundamental and inevitable element in the theory of strong interactions and it has enjoyed great success in medium energy phenomenology. More basic theories are expected to lead to Regge behaviour and in principle should allow the calculation of the trajectory and residue functions in terms of the fundamental parameters of the theory.

We thus describe the behaviour of the normal part of our amplitudes in Regge language. It is the logical and utilitarian language to use in the absence of more fundamental calculations.

As is well known, the classical Regge contributions involve a number of free parameters owing to the arbitrariness of the residues and of the form of the Regge cuts. However, the non-dominant Regge pole contributions decrease rapidly with energy and are almost negligible beyond ISR energies. Thus it turns out, as far as $F_{\pm}^{N}$ is concerned, that the gross features of the ISR regime and beyond largely require only its Pomeron (P) pole and P ⊗ P cut contributions. We take for these

$$F_{+}^{P}(s,t) = C_{p} e^{\beta_{p} t} [i - \cot(\tfrac{\pi}{2} \alpha_{p}(t))] s^{\alpha_{p}(t)} \tag{5.1}$$

and

$$F_{+}^{PP}(s,t) = C_{pp} e^{\beta_{pp} t} [i \sin(\tfrac{\pi}{2} \alpha_{pp}(t)) - \cos(\tfrac{\pi}{2} \alpha_{pp}(t))] \frac{s^{\alpha_{pp}(t)}}{\ell n(s e^{-i\pi/2})} , \tag{5.2}$$

where

$$\alpha_{p}(t) = 1 + \alpha_{p}' t \tag{5.3}$$

and

$$\alpha_{pp}(t) = 1 + \frac{1}{2} \alpha_{p}' t , \tag{5.4}$$

a description which involves only four free parameters (C_{p}, C_{pp}, β_{p}, β_{pp}), the slope α_{p}' being fixed at its conventional world-value

$$\alpha_{p}' = 0.25 \ (\mathrm{GeV})^{-2} . \tag{5.5}$$

The fine details at ISR energies are sensitive to the non-dominant Regge poles (R), so we have included them and have taken the form :

$$F_{+}^{R}(s,t) = C_{R}^{+} \gamma_{R}^{+}(t) e^{\beta_{R}^{+} t} [i - \cot(\tfrac{\pi}{2} \alpha_{R}^{+}(t))] \, s^{\alpha_{R}^{+}(t)} \tag{5.6}$$

and

$$F_{-}^{R}(s,t) = - C_{R}^{-} \gamma_{R}^{-}(t) e^{\beta_{R}^{-} t} [i + \tan(\tfrac{\pi}{2} \alpha_{R}^{-}(t))] \, s^{\alpha_{R}^{-}(t)} , \tag{5.7}$$

where

$$\alpha_R^{\pm}(t) = \alpha_R^{\pm}(0) + \alpha' t \qquad (5.8)$$

and

$$\gamma_R^{\pm}(t) = \frac{\alpha_R^{\pm}(t)[\alpha_R^{\pm}(t)+1][\alpha_R^{\pm}(t)+2]}{\alpha_R^{\pm}(0)[\alpha_R^{\pm}(0)+1][\alpha_R^{\pm}(0)+2]}, \qquad (5.9)$$

the parameter α' being fixed at the usual phenomenological value

$$\alpha' = 0.88\ (\mathrm{GeV})^{-2}. \qquad (5.10)$$

The huge amount of data in the region $\sqrt{s} = 10$ GeV up to the ISR also probes the R ⊗ P cuts, taken to have the simple form [see ref. 20] :

$$F_+^{RP}(s,t) = t^2 C_{RP}^+ e^{\beta_{RP}^+ t}\left[1 \sin\left(\frac{\pi}{2}\alpha_{RP}^+(t)\right) - \cos\left(\frac{\pi}{2}\alpha_{RP}^+(t)\right)\right] \frac{s^{\alpha_{RP}^+(t)}}{\ell n(s e^{-i\pi/2})} \qquad (5.11)$$

and

$$F_-^{RP}(s,t) = t^2 C_{RP}^- e^{\beta_{RP}^- t}\left[\sin\left(\frac{\pi}{2}\alpha_{RP}^-(t)\right) + i \cos\left(\frac{\pi}{2}\alpha_{RP}^-(t)\right)\right] \frac{s^{\alpha_{RP}^-(t)}}{\ell n(s e^{-i\pi/2})}, \qquad (5.12)$$

where

$$\alpha_{RP}^{\pm}(t) = \alpha_{RP}^{\pm}(0) + \alpha'_{RP} t\ , \qquad (5.13)$$

and

$$\alpha'_{RP} = \frac{\alpha' \alpha'_P}{\alpha' + \alpha'_P} = 0.19\ (\mathrm{GeV})^{-2}\ . \qquad (5.14)$$

The parameters $\alpha_{RP}^{\pm}(0)$ are left free, the RP cuts being considered as effective cuts in describing the complicated lower energy region. (The dimensional scale factor $s_0 = 1$ GeV^2 has been left out in writing eqs. (5.1)-(5.2), (5.6)-(5.7) and (5.11)-(5.12).)

We have also considered the effect upon our parametrisation of attempting to fit the low-energy data in the range $4.5 \lesssim \sqrt{s} \lesssim 10$ GeV. The inclusion of the numerous and very precise forward data at low-energies poses no problem. It is sufficient to include a supplementary low-intercept exchange-degenerate Regge term $\tilde{R}$ of the form (5.6)-(5.9), i.e. with

$$C_{\tilde{R}}^{+} = C_{\tilde{R}}^{-} \equiv C_{\tilde{R}} , \quad \beta_{\tilde{R}}^{+} = \beta_{\tilde{R}}^{-} \equiv \beta_{\tilde{R}}, \quad \alpha_{\tilde{R}}^{+} = \alpha_{\tilde{R}}^{-} \equiv \alpha_{\tilde{R}} \tag{5.15}$$

and

$$\gamma_{\tilde{R}}^{+} = \gamma_{\tilde{R}}^{-} = \frac{[\alpha_{\tilde{R}}(t) + 1][\alpha_{\tilde{R}}(t) + 2][\alpha_{\tilde{R}}(t) + 3]}{[\alpha_{\tilde{R}}(0) + 1][\alpha_{\tilde{R}}(0) + 2][\alpha_{\tilde{R}}(0) + 3]} , \tag{5.16}$$

α' being fixed at the previous value 0.88 $(\text{GeV})^{-2}$.

The inclusion of the non-forward data at low energies is somewhat more complex and is beyond the scope of this paper. It would require a much more detailed analysis of the Regge contributions*.

Our insistence on the necessity of studying the entire medium and high energy regime inevitably implies that we have many free parameters. But there is a huge number of data points which we succeed in describing accurately and the parameters are well determined.

Even if the ultimate details of our Regge parametrisations may be open to slight modifications the asymptotic behaviour seems to be stable and the persisting difference between pp and $\bar{p}p$ at very high energies appears to be independent of such details.

---

* In this connection it should be noted that, to our knowledge, there is no theoretical treatment in the literature which accounts for the relatively recent and highly accurate $\bar{p}p$ data in the lower energy region.

6. COMPARISON WITH EXPERIMENTAL DATA

The amplitudes (3.15), (3.16), (5.1)-(5.16) were used to fit a total number of 582 experimental data points (112 in the forward direction [21,22] - σ_T, ρ, $\Delta\sigma$ for $\sqrt{s} \gtrsim 4.5$ GeV and 470 in the non-forward direction [1-3, 23, 24] - $d\sigma/dt$ for $\sqrt{s} \gtrsim 10$ GeV). The best-fit parameters are shown in Table I.

The corresponding χ^2 is $\simeq 2.5$/point, a very satisfactory value, bearing in mind that we did not introduce any normalization corrections in connection with the experimental values. The partial χ^2 at $t = 0$ is $\simeq 1.1$/point. The quality of the fit can be seen in figs. 1-7.

We wish to draw attention to several aspects of our fit to the present data.

As can be seen from figs. 5-7 we have a very good description of the ISR and CERN-collider differential cross-sections. At $\sqrt{s} = 546$ GeV our value of $\sigma_{el}^{\bar{p}p}$ is 13.3 mb, to be compared with the experimental one [24] 13.3 ± 0.6 mb.

Note however that the presence of the Froissaron induces a slow <u>increase</u> of the slope of the diffraction peak towards $t=0$, while the experimental values are obtained by using the usual exponential extrapolations of $d\sigma/dt$ involving a <u>constant</u> slope. For example, our slope evaluated for $0.03 < |t| < 0.15$ GeV^2 is 15.5 (GeV)$^{-2}$, in agreement with the experimental value [24] in the same region of t, 15.2 ± 0.2 (GeV)$^{-2}$, whereas our value of the slope at $t=0$ (which is, of course, inaccessible experimentally) is 16.5 (GeV)$^{-2}$. The increase

of the slope towards small values of t is, in our approach, a finite-energy effect of the AKM theorem [18], which has firm theoretical grounds. Effects of this kind must be kept in mind in future, when measuring σ_T at Tevatron or SSC energies and care must therefore be exercised in drawing conclusions as to the analytic form of the s-dependence of σ_T. (Similar considerations are mentioned in ref. [25].)

Concerning our fit to the total cross-sections (fig. 1) we note that our value for $(1 + \rho^2_{\bar{p}p})\sigma^{\bar{p}p}_T$ at $\sqrt{s}$ = 546 GeV is 64.7 mb as compared with the experimental value [22] 63.3 ± 1.5 ± 0.6 mb. Using our predicted value 0.115 for ρ^-_{pp}, we obtain $\sigma^{\bar{p}p}_T$ = 63.9 mb, compatible with the value deduced from experiment $\sigma^{\bar{p}p}_T$ = 62.4 ± 2.1 mb (the value quoted by the UA4 Collaboration [22] $\sigma^{\bar{p}p}_T$ = 61.9 ± 2.1 mb is obtained by assuming that ρ^-_{pp} = 0.15).

Recently, using the $\bar{S}$ppS collider in a pulsed mode the ratio of $\sigma^{\bar{p}p}_{inel}(\sqrt{s}$ = 900 GeV) to $\sigma^{\bar{p}p}_{inel}(\sqrt{s}$ = 200 GeV) has been measured to be 1.20 ± 0.01 ± 0.02 [26]. Using our formulae for $\sigma^{\bar{p}p}_T$ and $\sigma^{\bar{p}p}_{el}$ we find the value 1.27 for this ratio. It is not clear whether this discrepancy is significant or not. The Tevatron data should settle this question.

It is of interest to note that our results at $\sqrt{s}$ = 30 TeV (b_{pp} = 26.5 $(GeV)^{-2}$, σ^{pp}_T = 127 mb) fall within the allowed domain of values estimated from cosmic ray data [26,27] by Gaisser, Sukhatme and Yodh (see fig. 7 of ref. 29 which shows the variation of the proton-air inelastic cross-section $\sigma^{p\text{-air}}_{inel}$ with σ^{pp}_T for fixed values of the elastic slope parameter).

A second point of importance concerns $\Delta\sigma$. The presence of the odderon induces a minimum in $\Delta\sigma$ at $\sqrt{s} \simeq 100$ GeV followed by a slow ln s increase. This new effect occurs at energies beyond those of present experiments were $\Delta\sigma$ is measured, but it induces a curvature in $\Delta\sigma$ which is compatible with the present data (see fig. 2), even if it is not required by them. The effect is small and its detection requires very precise measurements of σ_T for both $\bar{p}p$ and pp in the TeV range of energies. However, the odderon effects are very important in $d\sigma/dt$ for sufficiently high t already at present day energies, as discussed in the following sections. We thus conclude that the best way to detect the effect of the odderon experimentally is via measurements in the non-forward region.

Similar considerations apply to the ratio ρ. The presence of the odderon induces a crossing between $\rho_{\bar{p}p}$ and ρ_{pp} at $\sqrt{s} \simeq 80$ GeV (see fig. 3), i.e. a change of sign of the difference $\rho_{\bar{p}p} - \rho_{pp}$. Again, the detection of these interesting effects, which lie beyond the present experimental range where this difference has been measured, will demand very precise measurements. It is important to note however that an indication of these effects can be obtained even if only $\rho_{\bar{p}p}$ (or only ρ_{pp}) is measured, by comparing experiment with the values obtained from a dispersion relation calculation with or without an odderon contribution. As we already said, we predict $\rho_{\bar{p}p} = 0.115$ at $\sqrt{s} = 546$ GeV.

As regards the CERN-collider data on $d\sigma/dt$, it should be noted that besides the data at $\sqrt{s} = 546$ GeV [2] there are also data at $\sqrt{s} = 630$ GeV [3] which confirm the presence of a break at $|t| \simeq 0.9$ GeV^2 followed by a shoulder. However, these data are available only for relatively high t values, $0.7 \lesssim |t| \lesssim 2.2$ GeV^2, and therefore the normalization is uncertain (estimated at $\pm$ 15%). We therefore did not use these data in our fit. Instead we present in fig. 6 the extrapolation of our fit to $\sqrt{s} = 630$ GeV and, for comparison, the results of refs. [6] and [30].

It should be noted that our amplitudes are rather tightly constrained, despite the number of parameters. The shoulder in $(d\sigma/dt)^{\bar{p}p}$ at ISR energies, the dip in $(d\sigma/dt)^{pp}$ at the same energies and the shape of $(d\sigma/dt)^{\bar{p}p}$ beyond the shoulder at CERN-collider energies are strongly correlated and it is difficult to modify one feature without destroying the fit to the others.

Finally, we show in fig. 4 the pp and $\bar{p}p$ differential cross-sections at $\sqrt{s}$ = 10 GeV. They are well fitted and we reproduce perfectly the interchange of dip and shoulder between pp and $\bar{p}p$ as the energy increases from $\sqrt{s}$ = 10 GeV up to ISR energies.

7. PREDICTIONS IN THE TeV ENERGY RANGE AND BEYOND

7.1. PREDICTIONS AT TEVATRON ENERGIES

Data will soon be available at $\sqrt{s} = 1.6$ TeV and at $\sqrt{s} = 1.86$ TeV at the Tevatron collider. Our predicted values for the forward observables are the following :

at $\sqrt{s} = 1.6$ TeV,

$$\sigma_T^{\bar{p}p} = 77.9 \text{ mb}, \quad \sigma_T^{pp} = 75.7 \text{ mb},$$
$$\rho_{\bar{p}p} = 0.104 \quad , \quad \rho_{pp} = 0.186 \tag{7.1}$$

and at $\sqrt{s} = 1.86$ TeV,

$$\sigma_T^{\bar{p}p} = 80.1 \text{ mb}, \quad \sigma_T^{pp} = 77.8 \text{ mb},$$
$$\rho_{\bar{p}p} = 0.102 \quad , \quad \rho_{pp} = 0.188 \ . \tag{7.2}$$

Our predictions for the $\bar{p}p$ and pp differential cross-sections at Tevatron energies are shown in fig. 7, where they are compared with the curve for $\sqrt{s} = 546$ GeV.

As already mentioned, for small t the $d\sigma/dt$'s are essentially equal because F_+ dominates and $F_{\bar{p}p} \simeq F_{pp}$. For sufficiently high t ($|t| \gtrsim 1.2$ GeV^2) we again have almost equal $d\sigma/dt$'s, but now because F_- dominates and $F_{\bar{p}p} \simeq -F_{pp}$. We note from Fig. 7 that the structure between these two regions of t becomes more and more complex with energy :

i) The dip in pp sharpens and moves towards smaller t roughly like $1/\ell n^2 s$, while $\bar{p}p$ begins anew to develop a dip‡ which also moves inwards roughly like $1/\ell n^2 s$. The fact that the movement of the dip is not exactly $1/\ell n^2 s$ indicates that the asymptotic regime is very remote.

‡ Note that this dip reappears at a much higher energy than that emerging from the more constrained analysis given in the last reference of ref. 5, in the framework of the same theoretical ideas as used here.

ii) The difference between the two $(d\sigma/dt)$'s shows an increasing number of oscillations and is quite significant.

For completeness, we also quote the predicted values for the forward slope $b\,(s,t\neq 0)$ and for σ_{el} at Tevatron energies :

at $\sqrt{s} = 1.6$ TeV,

$$b_{\bar{p}p} = 18.6\ (\mathrm{GeV})^{-2}\ ,\ b_{pp} = 18.8\ (\mathrm{GeV})^{-2}\ ,$$
$$\sigma_{el}^{\bar{p}p} = 17.5\ \mathrm{mb}\ ,\ \sigma_{el}^{pp} = 16.6\ \mathrm{mb} \qquad (7.3)$$

and at $\sqrt{s} = 1.86$ TeV,

$$b_{\bar{p}p} = 18.9\ (\mathrm{GeV})^{-2}\ ,\ b_{pp} = 19.1\ (\mathrm{GeV})^{-2}\ ,$$
$$\sigma_{el}^{\bar{p}p} = 18.1\ \mathrm{mb}\ ,\ \sigma_{el}^{pp} = 17.2\ \mathrm{mb}. \qquad (7.4)$$

7.2. PREDICTIONS AT SSC ENERGIES

The magnificent SSC project, if accomplished, will provide crucial tests for the new effects implied in our model theory. At $\sqrt{s} = 40$ TeV, we predict the following values :

$$\sigma_T^{\bar{p}p} = 136.5\ \mathrm{mb}\ ,\ \sigma_T^{pp} = 133.0\ \mathrm{mb}\ ,$$
$$\rho_{\bar{p}p} = 0.061\ ,\ \rho_{pp} = 0.196,$$
$$b_{\bar{p}p} = 26.9\ (\mathrm{GeV})^{-2}\ ,\ b_{pp} = 27.4\ (\mathrm{GeV})^{-2}, \qquad (7.5)$$
$$\sigma_{el}^{\bar{p}p} = 35.4\ \mathrm{mb}\ ,\ \sigma_{el}^{pp} = 33.7\ \mathrm{mb}\ .$$

The predictions for the $d\sigma/dt$'s at $\sqrt{s} = 40$ TeV are shown in fig. 8, where we also show the curve at $\sqrt{s} = 17$ TeV (the energy corresponding to the proposed LHC project which utilizes the LEP tunnel). The phenomenon of activity in the dip region

discussed above is accentuated at SSC energies. It is clear that a comparison of pp and $\bar{p}p$ scattering remains of great interest even at these extremely high energies.

7.3. ASYMPTOPIA

We have already mentioned that "true asymptopia", the region where all amplitudes are dominated by their leading terms, is very far away indeed. This is illustrated quantitatively in figs. 9-12 where σ_T, σ_{el}, σ_{el}/σ_T, $\Delta\sigma$ and ρ are shown in the range 10 GeV $\leq \sqrt{s} \leq 10^{19}$ GeV. The slowness of the approach to asymptopia at t=0 is clearly indicated by comparing ρ_{pp} and $\rho_{\bar{p}p}$ at SSC energies with their truly asymptotic limits of $\pm$ 0.11.

Of course this does not mean that the asymptotic terms $F_{\pm}^{AS}$ do not show themselves at present-day energies. For example the growth of σ_T is an obvious manifestation of the Froissaron type behaviour in F_+, even though the Pomeron contribution in F_+^N remains relatively large up to $\sqrt{s}$ = 1000 TeV.

In the case of F_- the situation is much more spectacular, and truly asymptotic effects show themselves rather early in energy as a result of the odderon dominance for t values beyond the diffraction dip. As demonstrated in our study, these manifest themselves in the range ISR-CERN-collider. The reason for this is clear. The "normal" terms in F_- correspond to the standard Regge vector-meson exchanges and thus disappear at least as rapidly as $1/\sqrt{s}$. One thus observes the consequences of the dominance of F_-^{AS} relatively early in energy.

As can be seen from fig. 13, where we show $(d\sigma/dt)^{\bar{p}p}$ at $\sqrt{s}$ = 0.053, 0.546, 1.8, 5, and 40 TeV, there is a rather complex variation of the $\bar{p}p$ differential cross-section in the shoulder region and beyond due to the odderon dominance. In the above range of energies and in this t-region, the O_1 term in (3.16) is negligible because of its fast decrease with t. The O_2 term is dominant for $|t_{dip}| < |t| < 2$ GeV^2, which results in an increase of $d\sigma/dt$ with energy. For $|t| \gtrsim 6$ GeV^2 the O_3 term becomes dominant and leads to the prediction $d\sigma/dt$ = const with energy. In between, the O_2 and O_3 terms interfere, leading to the effects seen at $\sqrt{s}$ = 40 TeV in fig. 13.

7.4. STRUCTURE AND EVOLUTION WITH THE ENERGY OF SCATTERING AMPLITUDES

The features discussed above can be simply understood from the structure and evolution with energy of the scattering amplitudes.

We show in figs. 14-17 the real and imaginary parts of the amplitudes (all divided by s) at four typical energies : $\sqrt{s}$ = 52.8 GeV (ISR), $\sqrt{s}$ = 546 GeV (CERN-collider), $\sqrt{s}$ = 1.8 TeV (Tevatron) and $\sqrt{s}$ = 40 TeV (SSC). The dominance of F_+ at small t is clearly visible at all these energies. The dominance of F_- for sufficiently high t begins to show itself already at ISR energies (fig. 14). It is clearly established at CERN-collider energies (fig. 15), while at Tevatron and SSC energies the amplitude F_+ is simply negligible in this region of t (figs. 16-17).

The appearance of a structure region in both $\bar{p}p$ and pp at moderate t is controlled by the zeros of the F_+ amplitude, which dominates for small t. The characteristics of this region (the sign and the zeros of the difference $(d\sigma/dt)^{\bar{p}p} - (d\sigma/dt)^{pp}$ and the movement of the dips towards smaller t with increasing energy)

can be directly understood form figs. 14-17. The structure region is the unavoidable consequence of a transition regime between the dominance of F_+ at small t and the dominance of F_- at sufficiently high t. It will remain a region of interest up to super-high energies. It is the basis of our insistence that it will always remain interesting to compare pp and $\bar{p}p$.

8. COMPARISON WITH OTHER MODELS

Most models of diffraction scattering are constructed so that the crossing-symmetric amplitude F_+ dominates at high energies for all t [30-32]. The contributions to F_- are usually Regge-like and consequently have largely disappeared by ISR energies. Hence these models predict equality of $(d\sigma/dt)^{\bar{p}p}$ and $(d\sigma/dt)^{pp}$, in serious contradiction with the ISR data. They cannot accomodate these data without the addition of a new dynamical mechanism analogous to the odderon.

There are three models in the literature which include a crossing-odd amplitude F_- that remains important at ISR energies.

In the model of Donnachie and Landshoff [6] the force responsible for this is three-gluon exchange calculated perturbatively. F_- dominates at large t for sufficiently high energies, as it does for us. However their F_- becomes constant at fixed t as $s \to \infty$ and, according to the authors, may well begin to decrease when higher order corrections are taken into account. In contrast, our maximal odderon F_-^{AS} grows at fixed t, in a certain t range beyond the shoulder region, as explained in the previous section. There is some evidence from the latest collider data [3] to support the picture of a growing F_-. The Tevatron data should test it even more clearly.

In Islam's work [7] the nucleon is visualized as a core of valence-quarks surrounded by a cloud of quark-antiquark pairs and it is argued that an odderon amplitude emerges when the cores interact by exchanging a $C = -1$ $u\bar{u} + d\bar{d}$ state while the clouds undergo maximal diffraction scattering [19]. This is interesting because it provides a dynamical picture for the origin of the odderon which links the $s\ \ell n^2 s$ behaviour in F_+ to the behaviour of F_-.

In a description based on perturbative Reggeon Field Theory, Dash and Jones have included a $C = -1$ odderon-like amplitude which is treated in a analogous fashion to the Pomeron [33].

Finally we note that Sukhatme has suggested that an odderon amplitude might emerge from the dual parton model [34].

It seems to us that the most relevant question is whether an odderon like amplitude can be shown to be compatible with QCD.

In the absence of a theoretical answer, we can at least test for the maximal odderon behaviour by searching experimentally at very high energies for what is a very characteristic signature, namely the continued growth with energy of the pp and $\bar{p}p$ differential cross-sections at fixed t in a certain region beyond the diffraction dip (see sect. 7).

9. CONCLUSIONS

We have constructed a model theory for the behaviour of strong interaction scattering amplitudes at high energies. The amplitudes respect all the rigorous general theorems on asymptotic growth and in a well defined sense saturate them : both the even and the odd under crossing amplitudes $F_{\pm}$ grow ultimately at the maximal permissible functional rate. We call this the "principle of maximal strength of the strong interactions".

The asymptotic behaviour at $t = 0$

$$F_{+}(s,0) \sim i\, s\, \ell n^2 s, \quad \text{as } s \to \infty \tag{9.1}$$

is an old idea but the so-called "maximal odderon" behaviour

$$F_{-}(s,0) \sim s\, \ell n^2 s, \text{ as } s \to \infty \tag{9.2}$$

is less well known.

We have argued, on the basis of our analysis of the pp and $\bar{p}p$ data from $\sqrt{s} \simeq 10$ GeV up to the CERN $S\bar{p}pS$ collider, that the odd-under-crossing amplitude increases with energy asymptotically and is varying in the "maximal odderon" fashion [3.16]. The difference between $(d\sigma/dt)^{pp}$ and $(d\sigma/dt)^{\bar{p}p}$ at the ISR, which proves unequivocally that F_{-} is still important at these energies, and the growth of the $\bar{p}p$ shoulder region between ISR and CERN collider play a vital role in demonstrating this assertion. With this behaviour we achieve an impressive fit to the pp and $\bar{p}p$ data in the range $10 \leqslant \sqrt{s} \leqslant 546$ GeV and $0 \leqslant -t \leqslant 2.5$ GeV^2.

The novelty of our interpretation implies unexpected and testable features at very high energies which were spelled out in detail in the Introduction. In particular we stressed that the growth with energy of the crossing-odd amplitude will be observable for values of t outside the diffraction peak and that this can be tested at the Tevatron collider.

Important, also, is the suggestion that the completely asymptotic behaviour only sets in at exceedingly high energies so that there will continue to be a measurable difference between $(d\sigma/dt)^{pp}$ and $(d\sigma/dt)^{\bar{p}p}$ in a narrow region surrounding the diffraction dip at all energies. This will provide an excellent test for these novel ideas.

In this connection a future collider with both pp and $\bar{p}p$ beams would be invaluable. A continued comparison of pp and $\bar{p}p$ is of great importance to an understanding of strong interaction dynamics.

Acknoledgements. The authors thank C. Bourrely, J. Dias de Deus, A. Donnachie, J. Fischer, M. Islam, P. Kroll, P.V. Landshoff, A. Martin, G. Matthiae, E. Predazzi and U. Sukhatme for useful discussions and correspondence, and their study was encouraged by the stimulating atmosphere of the Blois Workshop. One of us (E.L.) is grateful to Professors R. Vinh Mau and M. Giffon for their hospitality at the L.P.T.P.E., Université Pierre et Marie Curie, Paris VI and the I.P.N., Université Claude Bernard, Lyon respectively.

REFERENCES

[1] A. Breakstone et al., Phys. Rev. Lett. 54 (1985) 2180 ;
S. Erhan et al., Phys. Lett. 152B (1985) 131

[2] UA4 Collaboration, M. Bozzo et al., Phys. Lett. 155B (1985) 197

[3] UA4 Collaboration, M. Bozzo et al., Phys. Lett. 171B (1986) 142

[4] L. Łukaszuk and B. Nicolescu, Nuovo Cimento Lett. 8 (1973) 405 ;
K. Kang and B. Nicolescu, Phys. Rev. D11 (1975) 2461 ;
D. Joynson, E. Leader, C. Lopez and B. Nicolescu, Nuovo Cimento 30A (1975) 345

[5] P. Gauron and B. Nicolescu, Phys. Lett. 124B (1983) 429 ; 143B (1984) 253 ;
P. Gauron, E. Leader and B. Nicolescu, Phys. Rev. Lett. 52 (1984) 1952 ;
P. Gauron, E. Leader and B. Nicolescu, Phys. Rev. Lett. 54 (1985) 2656; 55(1985)639

[6] A. Donnachie and P.V. Landshoff, Nucl. Phys. B244 (1984) 322 ; DAMTP preprint 85/26 (1985) ; see also
A. Donnachie and P.V. Landshoff, in Proceedings of the 1st International Workshop on Elastic and Diffractive Scattering, Château de Blois, France, 3-6 June 1985 (Ed. Frontières, 1986), edited by B. Nicolescu and J. Tran Thanh Van, pp. 209-221

[7] M.M. Islam, T. Fearnley and J.P. Guillaud, Nuovo Cimento 81A (1984) 737

[8] A. Martin, in Proc. of the Blois Workshop, op. cit., pp. 153-163

[9] Y. Ya. Pomeranchuk, JETP 7 (1958) 499

[10] R.J. Eden, Phys. Rev. Lett. 16 (1966) 39 ;
T. Kinoshita, in Perspectives in Modern Physics, R.E. Marshak Ed. (Wyley and Sons, New York, 1966), p. 211 ;
G. Grunberg and Tran N. Truong, Phys. Rev. Lett. 31 (1973) 63 ; Phys. Rev. D9 (1974) 2874

[11] H. Cornille and A. Martin, Phys. Lett. 40B (1972) 671

[12] M. Froissart, Phys. Rev. 123 (1961) 1053 ;
A. Martin, Phys. Rev. 129 (1963) 1432 ;
A. Martin, Nuovo Cimento 42A (1966) 930

[13] L. Łukaszuk and A. Martin, Nuovo Cimento 52A (1967) 122

[14] S.M. Roy and V. Singh, Phys. Lett. 32B (1970) 50 ;
R.J. Eden, Rev. Mod. Phys. 43 (1971) 15

[15] J. Fischer, P. Kolar and I. Vrkoc, Phys. Rev. D13 (1976) 133 ;
J. Fischer, R. Saly and I. Vrkoc, Phys. Rev. D18 (1978) 4271 ;
J. Fischer, in Proc. of the International Europhysics Conference on High Energy Physics, Bari, Italy, 18-24 July 1985 (Laterza, Bari, 1985), edited by L. Nitti and G. Preparata, pp. 343-345

[16] J. Fischer, University of Bern preprint BUTP-86/15 (1986)

[17] G.F. Chew and S.C. Frautschi, Phys. Rev. Lett. 7 (1961) 394

[18] G. Auberson, T. Kinoshita and A. Martin, Phys. Rev. D3 (1971) 3185

[19] M.M. Islam, University of Connecticut preprint (1986)

[20] P.D.B.Collins and P.J. Kearney, Z. Phys. C22 (1984) 277

[21] W. Galbraith et al., Phys. Rev. 138 (1965) 913 ;
S.P. Denisov et al., Nucl. Phys. B65 (1973) 1 ;
A.S. Carroll et al., Phys. Lett. 80B (1979) 423 ;
K.J. Foley et al., Phys. Rev. Lett. 19 (1967) 857 ;
V. Blobel et al., Nucl. Phys. B69 (1974) 454 ;
P. Jenni et al. , Nucl . Phys. B129 (1977) 232 ;
G.G. Beznogikh et al., Phys. Lett. 39B (1972) 411 ;
D. Gross et al., Phys. Rev. Lett. 41 (1978) 217 ;

V. Bartenev et al., Phys. Rev. Lett. 31 (1973) 1367 ;
L.A. Fajardo et al., Phys. Rev. D24 (1981) 46 ;
CERN-Pisa-Rome-Stony Brook Collaboration, Phys. Lett. 62B (1976) 460 ;
U. Amaldi et al., Phys. Lett. 66B (1977) 390 ;
L. Baksay et al., Nucl. Phys. B141 (1978) 1 ;
U. Amaldi and K.R. Schubert, Nucl. Phys. B166 (1980) 301 ;
G. Carboni et al., Nucl. Phys. B254 (1985) 697 ;
N. Amos et al., Nucl. Phys. B262 (1985) 689

[22] UA4 Collaboration, M. Bozzo et al., Phys. Lett. 147B (1984) 392

[23] C.W. Akerlof et al., Phys. Rev. D14 (1976) 2864 ;
Z. Asa'd et al., Nucl. Phys. B255 (1985) 273 ;
R. Rubinstein et al., Phys. Rev. D30 (1984) 1413 ;
G. Fidecaro et al., Phys. Lett. B105 (1981) 309 ; Nucl. Phys. B173 (1980) 513 ;
E. Nagy et al., Nucl. Phys. B150 (1979) 221 ;
A. Breakstone et al., Nucl. Phys. B248 (1984) 253

[24] UA4 Collaboration, M. Bozzo et al., Phys. Lett. 147B (1984) 385

[25] M.M. Block and R.N. Cahn, Rev. Mod. Phys. 57 (1985) 563 ;
M.M. Block and R.N. Cahn, Phys. Lett. 168B (1986) 151

[26] UA5 collaboration, Z. Phys. C 32 (1986) 153

[27] T. Hara et al., Phys. Rev. Lett. 50 (1983) 2058

[28] R.M. Baltrusaitis, Phys. Rev. Lett. 52 (1984) 1380

[29] T.K. Gaisser, U.P. Sukhatme and G.B. Yodh, University of Maryland preprint PP-86-203 (1986);
G.B. Yodh, in Proc. of the Blois Workshop, op.cit., pp. 97-105

[30] C. Bourrely, J. Soffer and T.T. Wu, Phys. Rev. Lett. 54 (1985) 757

[31] H. Cheng and T.T. Wu, Phys. Rev. Lett. 24 (1970) 1456 ;
H. Cheng, J.K. Walker and T.T. Wu, Phys. Lett. 44B (1973) 97

[32] T.T. Chou and C.N. Yang, Phys. Rev. D19 (1979) 3268 ; Phys. Lett. 128B (1983) 457

[33] J.W. Dash and S.T. Jones, Phys. Rev. D33 (1986) 1512

[34] U.P. Sukhatme, in Proc. of the Blois Workshop, op. cit., pp. 195-200

TABLE 1

a) Froissaron parameters

F_1 mb	b_1^+ $(GeV)^{-2}$	F_2 mb	b_2^+ $(GeV)^{-2}$	F_3 mb	b_3^+ $(GeV)^{-2}$	R_+
0.29	4.25	-1.70	5.40	8.47	6.01	0.43

b) Odderon parameters

O_1 mb	b_1^- $(GeV)^{-2}$	O_2 mb	b_2^- $(GeV)^{-2}$	O_3 mb	b_3^- $(GeV)^{-2}$	R_-
0.031	7.02	-0.30	2.10	0.22	0.98	0.13

c) Regge parameters

	P	PP	R_+	R_-	$\tilde{R}$	$(RP)_+$	$(RP)_-$
$\alpha(0)$			0.54	0.41	-0.21	-0.19	-0.60
C, mb	29.4	-1.69	48.8	38.5	35.8	-4252.5	-937.4
β, $(GeV)^{-2}$	3.37	0.72	0.011	1.84	0.38	2.93	0.60

FIGURE CAPTIONS

Fig. 1 Data and theoretical curves for $\bar{p}p$ and pp total cross sections.

Fig. 2 Data and theoretical curve for $\Delta\sigma = \sigma_T^{\bar{p}p} - \sigma_T^{pp}$.

Fig. 3 Description of ρ = Re F(s,t=0)/Im F(s,t=0).

Fig. 4 Comparison between our results and the data on pp and $\bar{p}p$ differential cross sections at $\sqrt{s}$ = 9.8 GeV (the first two references in [23]).

Fig. 5 Comparison between our results and the ISR data on pp and $\bar{p}p$ differential cross sections ([1] and the last two references in [23]).

Fig. 6 Comparison between our results (GLN) and the CERN-collider data on $\bar{p}p$ differential cross sections [2,3,24] . Our curve at $\sqrt{s}$ = 630 GeV is a prediction. The results of refs. [6] (DL) and [30] (BSW) are also shown.

Fig. 7 Our prediction for the pp and $\bar{p}p$ differential cross sections at CERN-collider and Tevatron energies. The UA4 experimental results for $\bar{p}p$ at $\sqrt{s}$ = 0.546 TeV [2,24] are also shown.

Fig. 8 Our prediction for the pp and $\bar{p}p$ differential cross sections at LHC and SSC energies.

Fig. 9 Plot of $\sigma_T^{\bar{p}p}$ and $\sigma_{el}^{\bar{p}p}$ for $10 \leq \sqrt{s} \leq 10^{19}$ GeV.

Fig. 10 Plot of σ_{el}/σ_T for $10 \leq \sqrt{s} \leq 10^{19}$ GeV.

Fig. 11 Plot of $\Delta\sigma$ for $10 \leq \sqrt{s} \leq 10^{19}$ GeV.

Fig. 12 Plot of ρ for $10 \leq \sqrt{s} \leq 10^{19}$ GeV.

Fig. 13 Illustration of odderon effects beyond the structure region in $\bar{p}p$ differential cross section from ISR to SSC energies.

Fig. 14 The behaviour of the real and imaginary parts of the crossing-even and crossing-odd amplitudes (all divided by s) at the ISR energy $\sqrt{s}$ = 52.8 GeV.

Fig. 15 The same quantities as in fig. 14 at the CERN-collider energy $\sqrt{s}$ = 546 GeV.

Fig. 16 The same quantities as in fig. 14 at the Tevatron energy $\sqrt{s}$ = 1.6 TeV.

Fig. 17 The same quantities as in fig. 14 at the SSC energy $\sqrt{s}$ = 40 TeV.

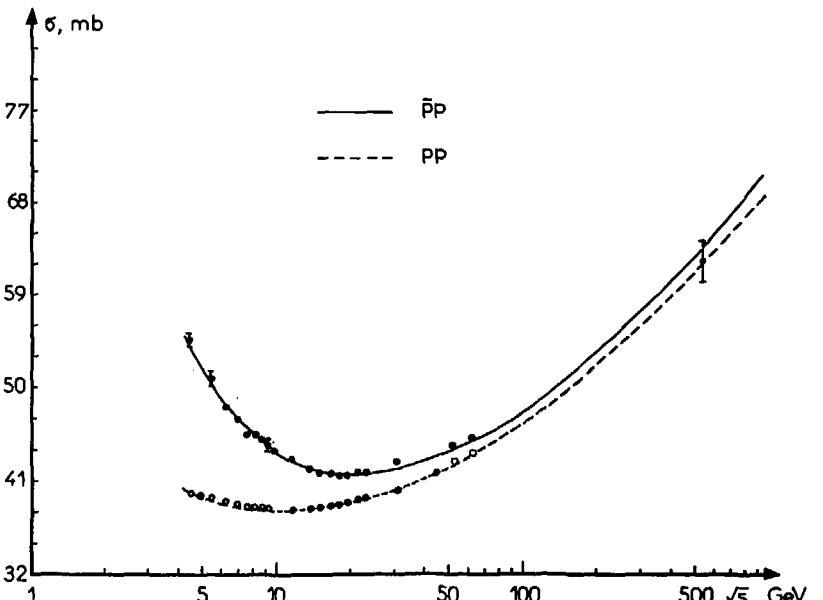

Fig. 1

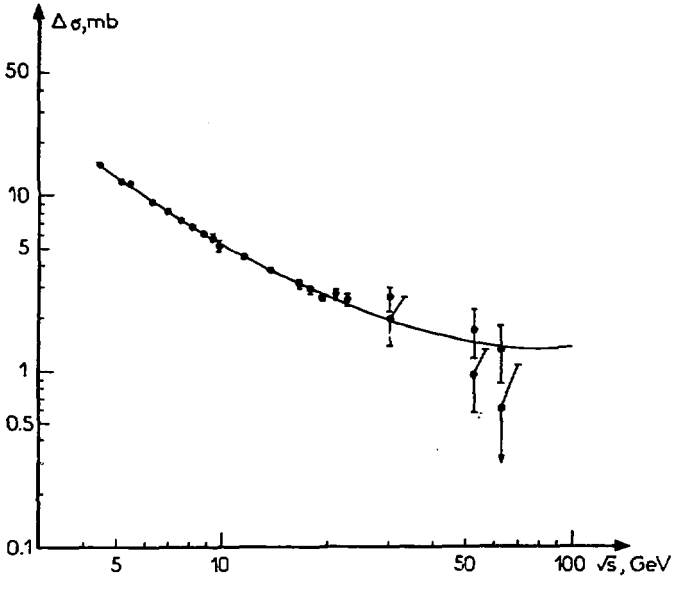

Fig. 2

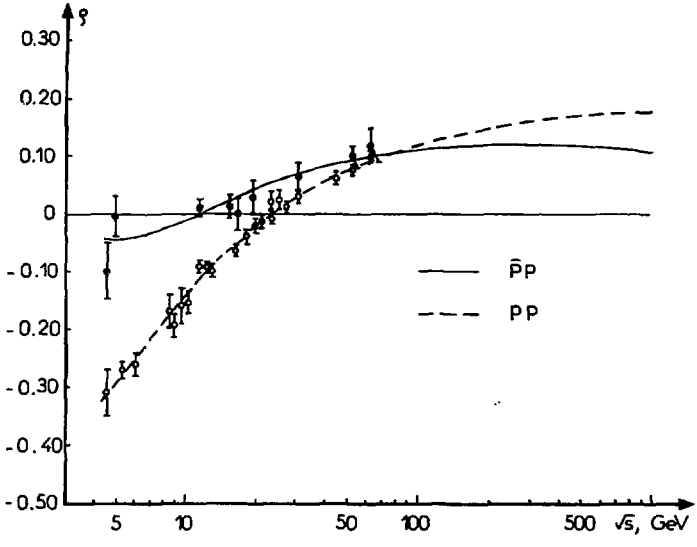

Fig. 3

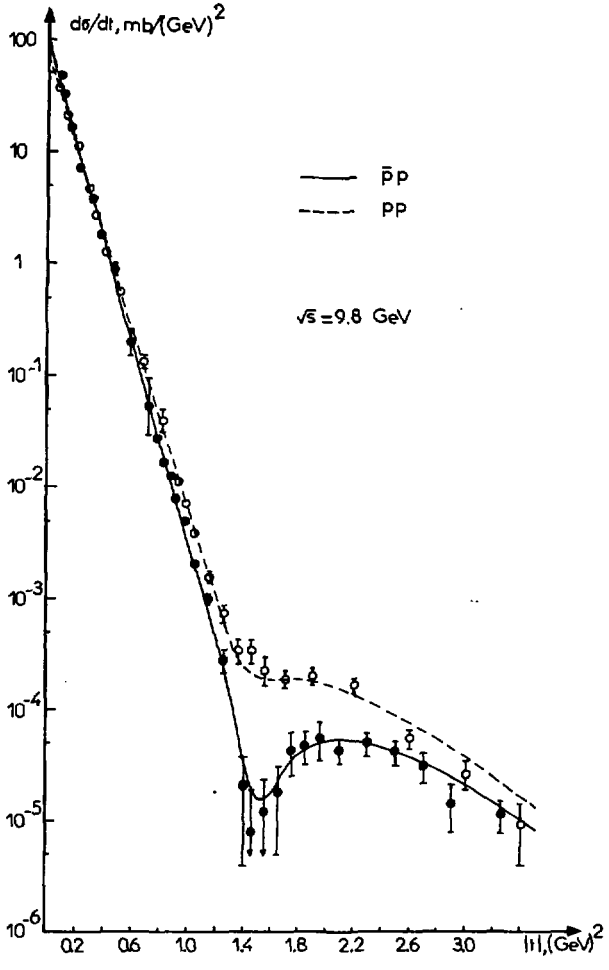
dσ/dt, mb/(GeV)²
100
10
1
10⁻¹
10⁻²
10⁻³
10⁻⁴
10⁻⁵
10⁻⁶
p̄p
pp
√s = 9.8 GeV
0.2
0.6
1.0
1.4
1.8
2.2
2.6
3.0
|t|,(GeV)²

Fig. 4

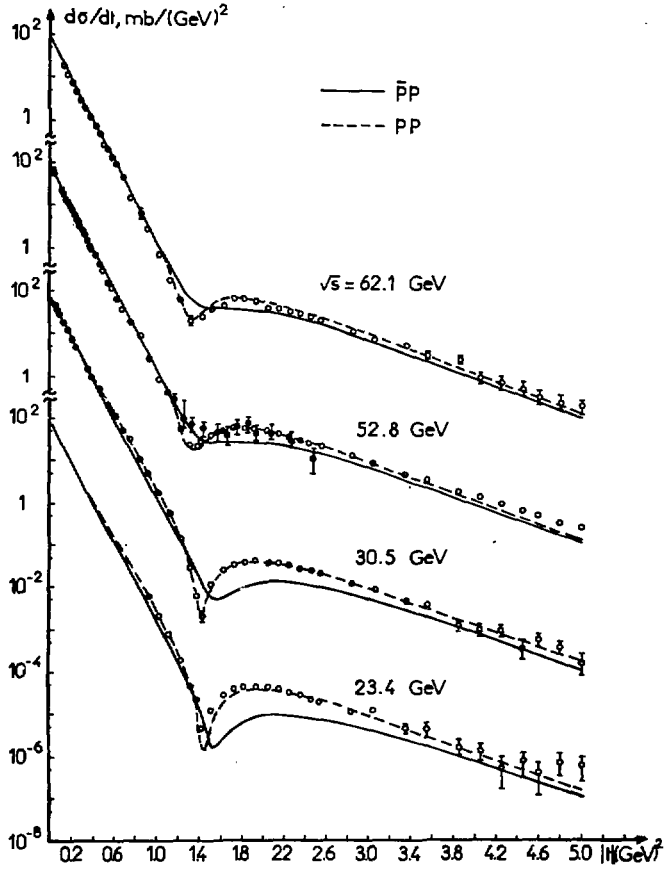
dσ/dt, mb/(GeV)²
10^2
1
10^{-2}
10^{-4}
10^{-6}
10^{-8}
$\bar{P}P$
PP
√s = 62.1 GeV
52.8 GeV
30.5 GeV
23.4 GeV
0.2 0.6 1.0 1.4 1.8 2.2 2.6 3.0 3.4 3.8 4.2 4.6 5.0 |t|(GeV)²

Fig. 5

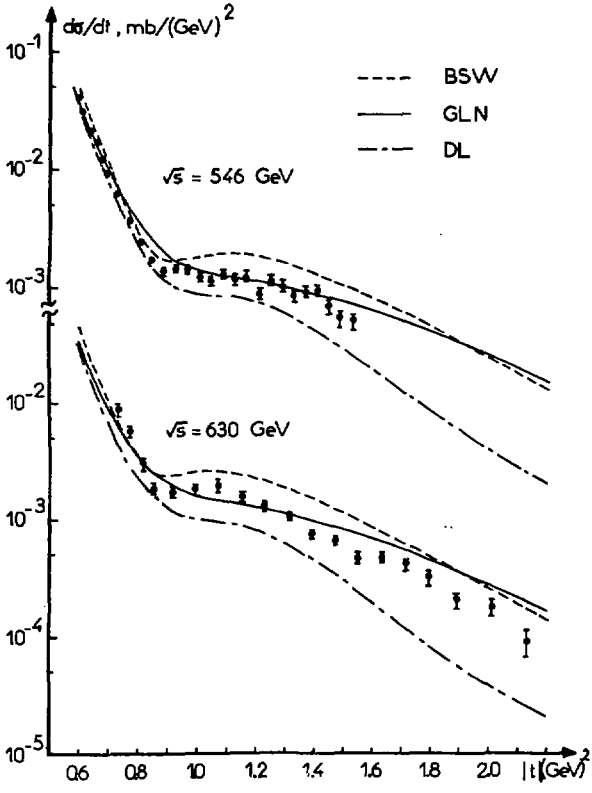
dσ/dt , mb/(GeV)^2
BSW
GLN
DL
$\sqrt{s}$ = 546 GeV
$\sqrt{s}$ = 630 GeV
10^{-1}
10^{-2}
10^{-3}
10^{-2}
10^{-3}
10^{-4}
10^{-5}
0.6
0.8
1.0
1.2
1.4
1.6
1.8
2.0
|t|(GeV)^2

Fig. 6

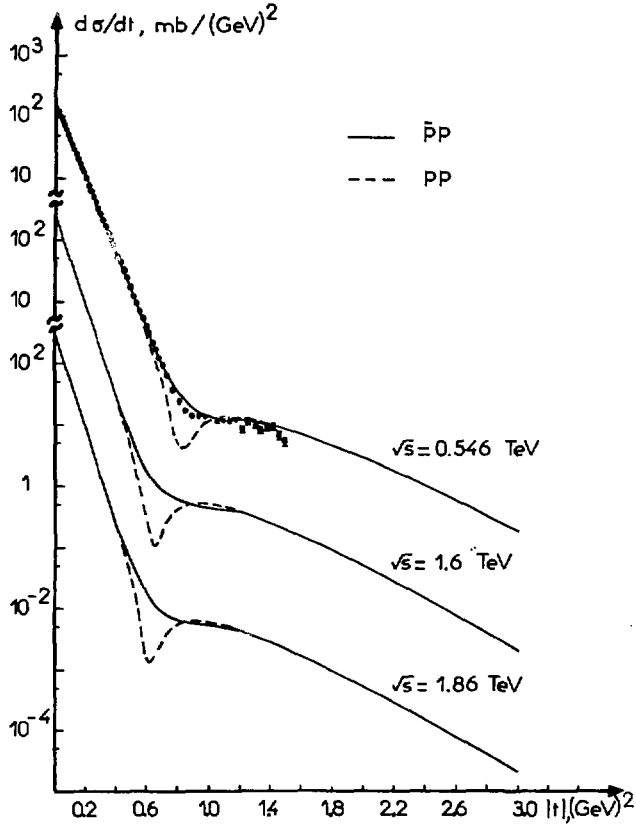
dσ/dt, mb/(GeV)²
10³
10²
10
10²
10
10²
1
10⁻²
10⁻⁴
p̄p
pp
√s = 0.546 TeV
√s = 1.6 TeV
√s = 1.86 TeV
0.2
0.6
1.0
1.4
1.8
2.2
2.6
3.0
|t|,(GeV)²

Fig. 7

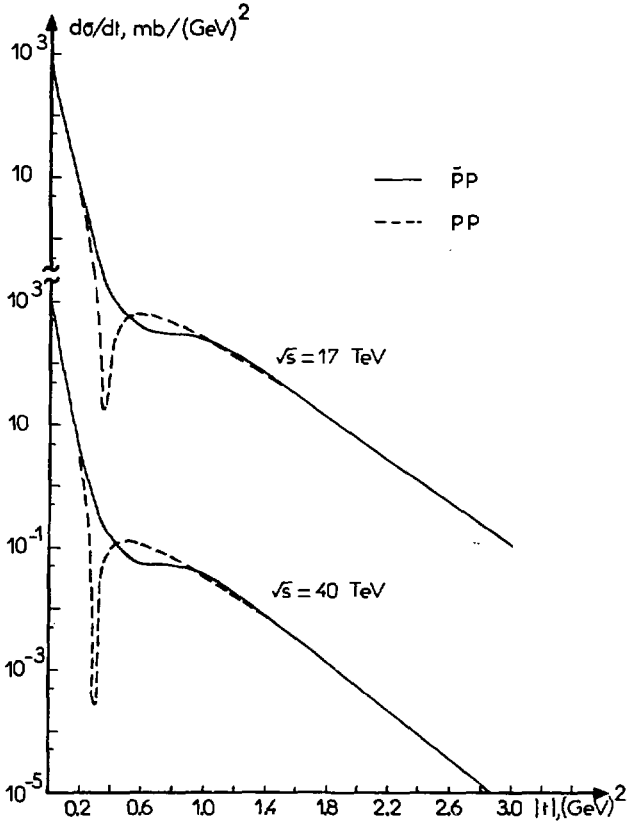
dσ/dt, mb/(GeV)^2
10^3
10
10^3
10
10^{-1}
10^{-3}
10^{-5}
$\bar{p}p$
pp
$\sqrt{s} = 17$ TeV
$\sqrt{s} = 40$ TeV
0.2
0.6
1.0
1.4
1.8
2.2
2.6
3.0
$|t|$,(GeV)^2

Fig. 8

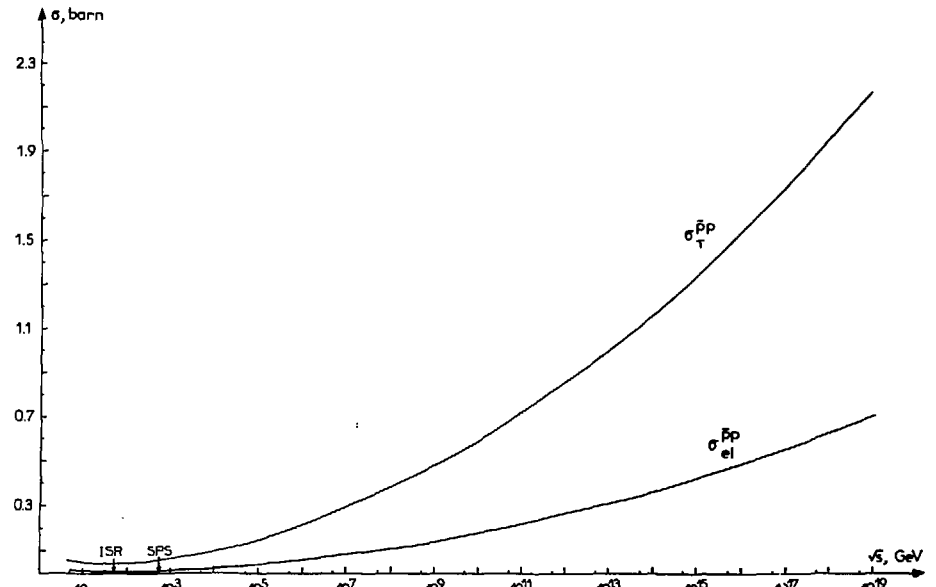
σ, barn
2.3
1.9
1.5
1.1
0.7
0.3
$\sigma_T^{\bar{p}p}$
$\sigma_{el}^{\bar{p}p}$
ISR
SPS
√s, GeV
10
10^3
10^5
10^7
10^9
10^{11}
10^{13}
10^{15}
10^{17}
10^{19}

Fig. 9

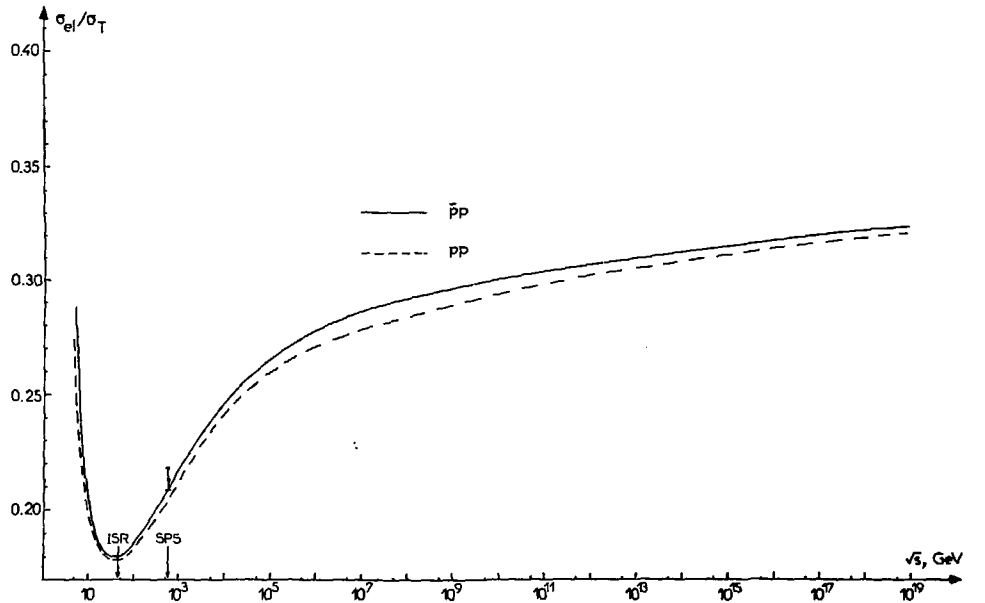
σ_{el}/σ_T
0.40
0.35
0.30
0.25
0.20
$\bar{p}p$
pp
ISR
SPS
$\sqrt{s}$, GeV
10
10^3
10^5
10^7
10^9
10^{11}
10^{13}
10^{15}
10^{17}
10^{19}

Fig. 10

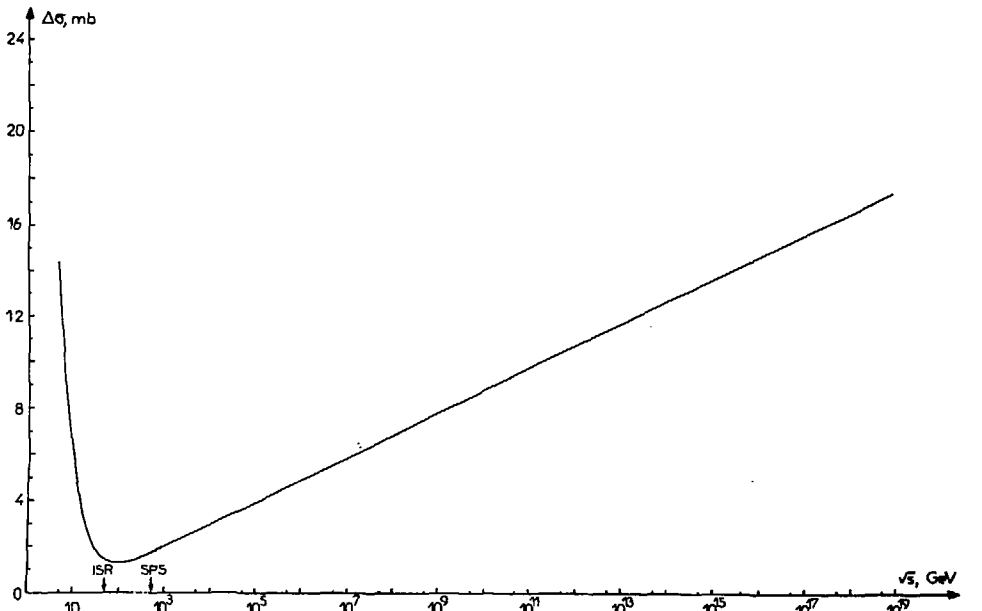
Δσ, mb
24
20
16
12
8
4
0
ISR
SPS
√s, GeV
10
10³
10⁵
10⁷
10⁹
10¹¹
10¹³
10¹⁵
10¹⁷
10¹⁹

Fig. 11

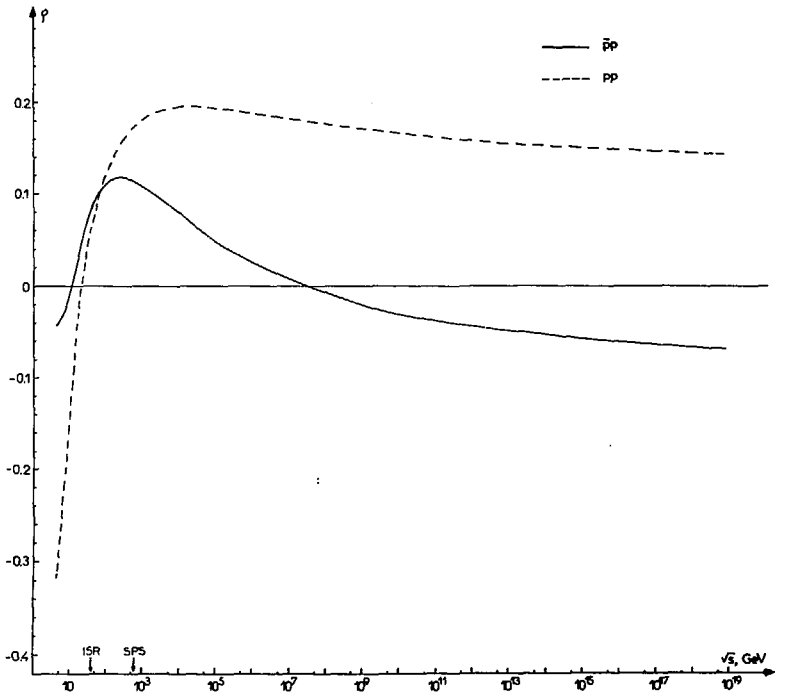
ρ
p̄p
pp
0.2
0.1
0
-0.1
-0.2
-0.3
-0.4
ISR
SPS
√s, GeV
10
10³
10⁵
10⁷
10⁹
10¹¹
10¹³
10¹⁵
10¹⁷
10¹⁹

Fig. 12

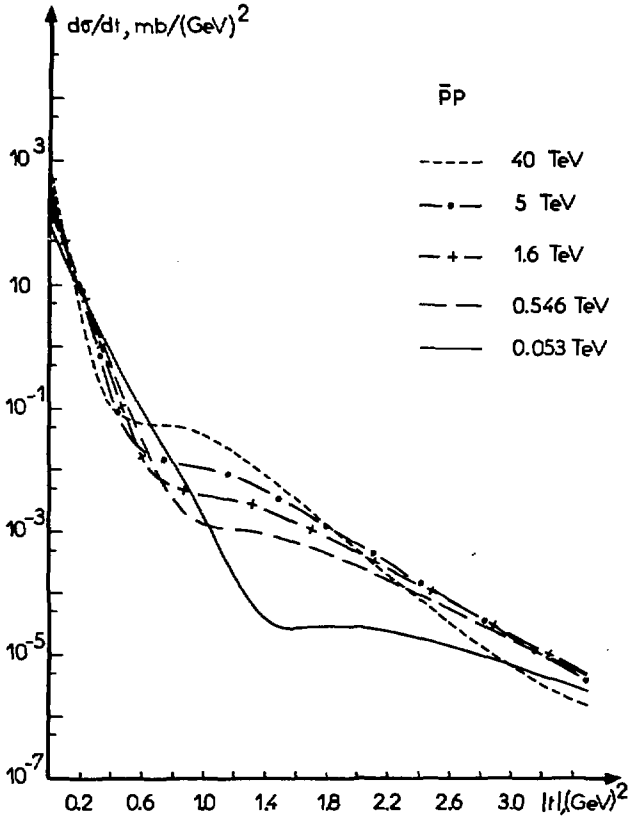
dσ/dt, mb/(GeV)^2
$\bar{p}p$
40 TeV
5 TeV
1.6 TeV
0.546 TeV
0.053 TeV
10^3
10
10^{-1}
10^{-3}
10^{-5}
10^{-7}
0.2
0.6
1.0
1.4
1.8
2.2
2.6
3.0
$|t|$,(GeV)^2

Fig. 13

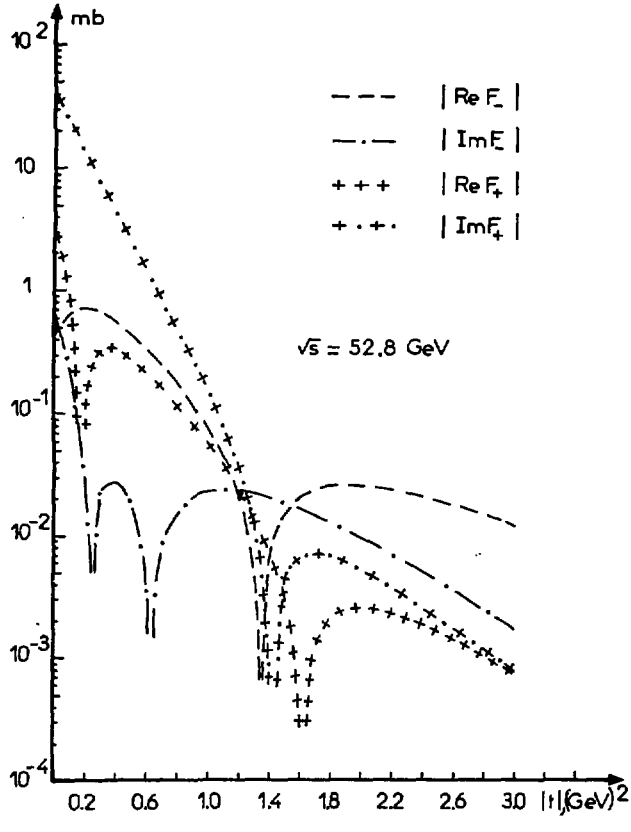
mb
10^2
10
1
10^{-1}
10^{-2}
10^{-3}
10^{-4}
| Re F_ |
| Im F_ |
| Re F+ |
| Im F+ |
√s = 52.8 GeV
0.2
0.6
1.0
1.4
1.8
2.2
2.6
3.0
|t|(GeV)^2

Fig. 14

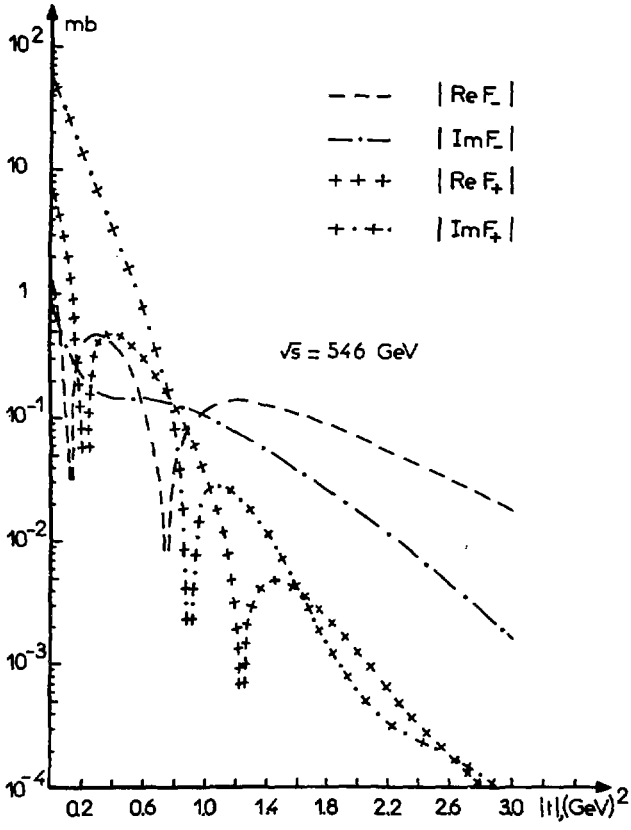
mb
10^2
10
1
10^{-1}
10^{-2}
10^{-3}
10^{-4}
0.2
0.6
1.0
1.4
1.8
2.2
2.6
3.0
$|t|,(GeV)^2$
$|ReF_-|$
$|ImF_-|$
$|ReF_+|$
$|ImF_+|$
$\sqrt{s} = 546$ GeV

Fig. 15

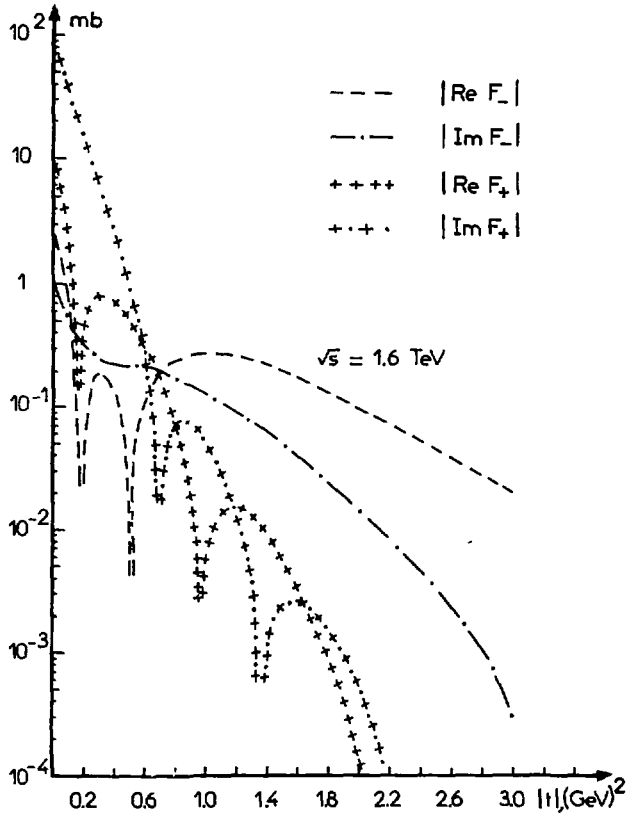
mb
10^2
10
1
10^{-1}
10^{-2}
10^{-3}
10^{-4}
|Re F_|
|Im F_|
|Re F+|
|Im F+|
√s = 1.6 TeV
0.2
0.6
1.0
1.4
1.8
2.2
2.6
3.0
|t|,(GeV)^2

Fig. 16

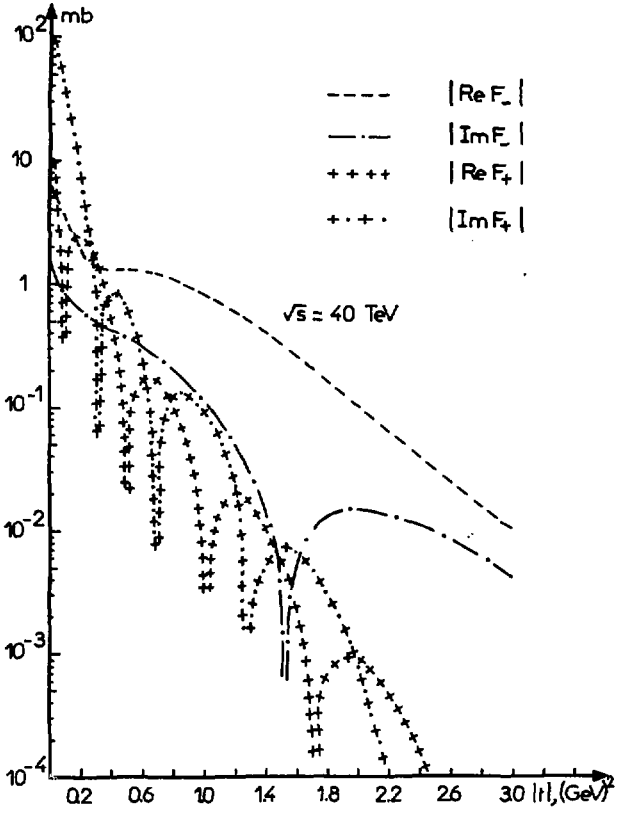
mb
10^2
10
1
10^{-1}
10^{-2}
10^{-3}
10^{-4}
$|Re F_-|$
$|Im F_-|$
$|Re F_+|$
$|Im F_+|$
$\sqrt{s} = 40$ TeV
0.2
0.6
1.0
1.4
1.8
2.2
2.6
3.0
$|t|, (GeV)^2$

Fig. 17